SHORT FATIGUE CRACKS AND CRACK CLOSURE

A. PINEAU*

ABSTRACT A survey of the literature devoted to short fatigue cracks is presented. The results obtained will natural short cracks initiated from inclusions or metallurgical defects are distinguished from those obtained more recently with artificial two-dimensional short cracks. The analytical difficulties encountered in the analysis of short cracks grown naturally, are underlined. The propagation of two-dimensional short cracks in fine grained materials can be rationalized in terms of crack closure effect, as shown by recent results which are given. A simple rule is proposed for estimating the resistance to short crack propagation from long crack data taking the R ratio effect into account. Limitations to this rule related to both metallurgical and environmental effects are briefly discussed.

INTRODUCTION

Considerable attention has been given recently to the growth behaviour of short fatigue cracks. A number of experimental results |1-14| have shown that short cracks ($\sim$ 0.05 - 0.5 mm) tend to propagate faster than long cracks ($\sim$ 5-20 mm). As a general rule this effect is noticed at low fatigue crack growth rates (F.C.G.R.), ($da/dN \simeq 10^{-6}$ mm/cycle) and low stress ratio ($R = K_{Min}/K_{Max} \simeq 0.10$).

Typical fatigue crack propagation curves are drawn in Fig. 1 for short and long cracks. Such a behaviour has been reported in several materials, including Al alloys |1,5|, low strength steels |3|, nodular cast iron |15|, Ni-Al bronze |11,12|, Ti alloy |10|. At low applied stress, a decrease of the short crack F.C.G.R. leading eventually to crack arrest is observed after an initial period corresponding to high propagation rate. At intermediate applied load, a minimum in short crack F.C.G.R. has been reported. At higher applied stress, the short crack F.C.G.R. are higher than those determined in specimens containing long cracks. In this figure, we have plotted the results in the conventional manner assuming that the ΔK expressions used for long and two-dimensionnal cracks do apply to short cracks, which is not necessarily the case as discussed in more detail later. The practical implication of the situation described in Fig. 1 is obvious since many engineering structures contain small cracks subjected to a low applied stress intensity factor range. In particular it is clear that if short cracks do propagate faster, the usual procedures for damage tolerance assessment based upon long crack behaviour are not necessarily conservative.

*Centre des Matériaux - Ecole des Mines de Paris
BP. 87 - 91003 EVRY CEDEX (FRANCE) - ERA CNRS N°767.

Another convenient way of presenting short crack data is shown in Fig. 2 where the stress range required to cause fatigue failure is plotted versus crack length. At zero crack length this stress range is equal to the endurance limit. The threshold stress intensity range (ΔK_{th}) measured in specimens containing long cracks is independent of crack length. The stress range ($\Delta K_{th} / \sqrt{\pi a}$) is then represented by a straight line of slope -0.5 on a log-log plot. Both lines intercept at a crack length defined by El Haddad et al |2| as l_o. If short crack behaviour actually followed both these straight lines, a specimen containing initially no crack would have the same endurance limit than a specimen containing a crack of length l_o. This would imply that if a specimen was tested at its endurance limit or slightly above, cracks should initiate and propagate very quickly to length l_o. Observations performed in ferritic steels are shown in Fig. 3. It can be noticed that the data points fall on a curve between straight lines. In Fig. 3a, $l_o \simeq 0.10$ mm. It can also be seen that the experimental curve corresponds to the threshold line for a length $l_1 \simeq 0.5$ mm. At the endurance limit, l_1 is therefore an upper bound of the short crack domain. These data indicate that, in ferritic steels, the short crack effects extend over a physically wide range of crack lengths up to about 0.5 - 1 mm which is much larger than microstructural dimensions such as the grain size.

In the present paper, we review a number of experimental informations and accompanying interpretations on the fatigue growth behaviour of short cracks in engineering materials. This paper does not intend to be an exhaustive review since this has already been done recently by several authors, see eg. |8,16,17|. In this study, we would like to concentrate on key points to determine whether short cracks behave differently from long cracks or not. More specifically, we will emphasize the importance of the crack closure effect, since there is a growing consensus to recognize the crucial role played by this phenomenon. In this presentation, we will first discuss several relevant data related to "natural" short cracks. Then recent results obtained with "artificial" two-dimensional short cracks and related interpretations in terms of crack closure effect will be presented. At this point, the importance of metallurgical factors will be mentionned. Both parts deal with smooth specimens without stress concentrations although the same concepts could be applied to interpret features related to the fatigue growth behavior of short cracks initiated from notches.

NATURAL SHORT CRACKS BEHAVIOUR

Natural short cracks are, by definition, those which initiate in engineering materials from natural defects such as inclusions in wrought materials or micro-shrinkage porosities in cast materials. Ten years ago, detailed informations on the crack growth of tiny cracks initiated from inclusions in two Al alloys were published by Pearson |1|. The results obtained by this author on one of these alloys are shown in Fig. 4 where the dashed line shows that the F.C.G.R. of small surface cracks (0.010-0.5 mm) are larger than the F.C.G.R. determined on long through-section cracks. In this study the length of the microcracks was measured from the inspection of the specimen surface. As these microcracks are really three-dimensional, an assumption must be made to calculate ΔK. In this study it was assumed that the crack front adopted an equilibrium semi-elliptical or semi-circular shape. This assumption was verified in one specimen containing a centre-crack which had a depth of about 0.25 mm. A close examination of the results given approximately in Fig. 4 shows that there is no short crack effect anymore for such crack length. There is thus no guarantee that the crack front corresponds to the assumed equilibrium shape for smaller crack depths. In particular it is quite possible that the geometry of tiny cracks initiated from inclusions is actually associated with higher values of the stress intensity factor, as shown schematically in Fig. 5 where the section of a spherical inclusion is shown. In this figure we have drawn successive positions of the crack front and the schematic variations of the stress intensity factor at points A and B as a function of the crack dimensions a and c. This is only a schematic. A more quantitative analysis would require K solutions for K when c/a is large which are not available, see eg. |18,19|. In spite of this, it is clear that K_A can be much larger than K_B. It is quite conceivable that high crack growth rates could be measured for short crack lengths because the driving force is larger than expected from the determination of the crack length on the specimen surface until the crack front adopts an equilibrium shape.

To illustrate this three-dimensional aspect associated with natural short cracks, we have reproduced in Fig. 6 recent observations made on tiny cracks initiated from graphite nodules in nodular cast iron |15|. In this figure, we have drawn, using successive sections, the aspect of nodules and associated non-propagating microcracks. Using the K expressions for a circular crack, it was found that $K_A \simeq 3.10$ MPa.m½ and $K_B \simeq 2.60$ MPa.m½ for the arrested crack front geometry. These values are lower than those corresponding to the threshold of two-dimensional cracks of similar dimensions. The short crack behaviour in this material, high values of F.C.G.R. and eventual crack arrest for very small apparent crack lengths as in other materials |5,10,11|, is not necessarily anomalous. It is believed that this behaviour reflects largely the difficulties related to the calculations of ΔK associated with the three-dimensional aspect of the problem.

Fig. 5 is an oversimplified picture. It is conceivable that the crack front is such that very high values of K exist at the specimen surface with natural defects such as real inclusions or microshrikange porosities. The same conclusion applies to the experiments carried out by Kitagawa et al |3| with initiating pits, as indicated previously by Taylor |20|. In the absence of more sophisticated calculations taking into account the real crack front geometry, it seems difficult to conclude unambiguously that short cracks do correspond to a specific behaviour. This is the reason why it is relevant to review the results obtained with two-dimensional short cracks.

TWO-DIMENSIONAL SHORT CRACKS

Recent experiments carried out on specimens containing two-dimensional cracks showed unambiguously that short cracks do propagate faster especially in the near-threshold regime |9,15,21|. These short cracks were made artificially by machining specimens which contained initially long fatigue cracks. The results obtained by Romaniv et al |21| reported in Fig. 7 show that ΔK_{th} is reduced from 7.5 MPa.m½ to about 4.5 MPa.m½ in mild steel when the crack length is decreased from 2 mm to 0.3 mm. Very similar results obtained recently on a low alloy steel, (A508 steel), are shown in Fig. 8 where it can be seen that the threshold value is much smaller in specimens containing short cracks (0.3-0.5 mm) than in conventional CT or SEN type specimens |9|. This figure also shows that the short crack effect appears only for F.C.G.R. lower than approximately 10^{-5} mm/cycle. More recently, the threshold was determined at R = 0.10 as a function of crack length, using a similar procedure in nodular cast iron |15|. The results are given in Fig. 9 where it can be observed that the threshold is an increasing function of crack length over the 0.1 to 1 mm range. In those three examples where the F.C.G.R. determined on small crack specimens were compared to those measured with conventional long crack specimens, the short crack F.C.G.R. correspond, within a first approximation to an extrapolation of stage B of the Paris law (see Fig. 7 and 8). There exists also a break at very low FCGR in the da/dN-ΔK curves similar to that observed for long cracks but at smaller values of applied ΔK.

An explanation for this behaviour can be found in terms of crack closure. Since the work performed by Elber |22|, this phenomenon has been invoked to account for the influence of a number of parameters such as metallurgical factors or R effect on fatigue crack propagation. Crack closure is related to various physical and mechanical phenomena such as plasticity, oxidation, crack surface roughness behind the crack tip (see eg. |23|). It is therefore conceivable that crack closure effects depend on crack length, as clearly shown recently by two independent sets of experiments in which the material behind the crack tip was removed by machining |9,24|. Further measurements were made recently on nodular cast iron (Fig. 10). This figure shows that the opening stress intensity factor, K_{op}, is an increasing function of crack length over the 0.4 to 1.5 mm range. For crack lengths larger than 1.5 mm, it was observed that K_{op} was, within a first approximation, independent of crack length and equal to 4.1 MPa.m½. In A508 steel, |9| K_{op} was shown to be independent of crack length and K_{Max} for long cracks ($a \approx 20$ mm), as observed also by other investigators |25| in ferritic steels.

These results provide a basis for explaining short crack behaviour. For small crack lengths $K_{op} < K_{Min}$ and $\Delta K_{th} \rightarrow \Delta K_{th\ int}$ where $\Delta K_{th\ int}$ can be interpreted as an intrinsic property of the material. This value corresponds to the horizontal straight line drawn in Fig. 9 for $a \lesssim 0.15$ mm. For larger crack length, the effective $\Delta K = \Delta K_{eff} = K_{Max} - K_{op}(a)$ is lower than the applied $\Delta K = K_{Max} - K_{Min}$ when $K_{op} > K_{Min}$ but is larger than ΔK_{eff} determined for long cracks. In other words, about half the value of the threshold determined at low R ratios is due to crack closure while the other half is due to the "intrinsic" threshold in materials like nodular cast iron and A508 steel. In these materials, it was shown that the da/dN - ΔK_{eff} curve determined either on long or short crack specimens was unique. This clearly demonstrates that, in these situations where a proper calculation of ΔK can easily be made, the short crack problem is essentially associated with crack closure effect. The importance of crack closure on natural short cracks was also clearly shown by James and Morris |13| on a Ti alloy and Morris |26| on an Al alloy. It is felt that a proper account of the three-dimensional aspect of natural short cracks in conjunction with the influence of crack dimensions on crack closure could also explain the propagation behaviour of these small cracks including the crack arrest phenomenon.

The conclusion related to the effect of crack closure on short crack behaviour is similar to that reached by James and Smith |27| who have also worked on fine grained ferritic steels. It is an important conclusion, because it can provide a convenient practical approach for the assessment of short fatigue crack tolerance. In the absence of data on crack opening stress intensity factor, K_{op}, as a function of crack length, it can be assumed that $\Delta K_{th\ int}$ can be obtained by conducting experiments on long cracks tested at high R ratios. Fig. 11a illustrates the typical variations of ΔK_{th} as a function of the R ratio. Above a transition value R_t, there is a plateau which corresponds to a regime of R where crack closure effects are suppressed. It can easily be shown that for a long

crack, R_t is given by :

$$R_t^{\infty} = \frac{K^{\infty}_{op.}}{\Delta K_{th\ int} + K^{\infty}_{op}} \qquad (1)$$

where K^{∞}_{op} is the opening stress intensity factor for a long crack (Fig. 11b). For $R < R_t$, the variations of the threshold for long cracks ΔK^{∞}_{th} are given by :

$$\Delta K^{\infty}_{th} = (\Delta K_{th\ int} + K^{\infty}_{op})\,(1-R) \qquad (2)$$

This type of expression relating ΔK^{∞}_{th} to the R ratio is in broad agreement with a number of results published on steels, see eg. the results obtained by Cooke and Beevers |28| on pearlitic steels.

In many materials and especially in ferritic steels, the stage B of the Paris law corresponds to a regime where $K_{Max} >> K_{op}$ and $\Delta K_{applied}/\Delta K_{eff} \rightarrow 1$. Within a first approximation, the stage B of the Paris law can therefore be extrapolated linearly up to a final value corresponding to $\Delta K_{th\ int}$ as shown schematically in Fig. 11c when dealing with short cracks. This simple rule is likely to be conservative. It could provide a simple way for the assessment of short crack tolerance.

Another and complementary way of tackling the short crack problem would be to measure K_{op} as a function of crack length and to establish an experimental curve similar to that shown in Fig. 10 for nodular cast iron. If it is assumed that the $K_{op}(a)$ curve is not too drastically dependent on the loading conditions, at least for periodic loading, curves similar to those shown in Fig. 12 can easily be derived. These curves are drawn for illustration purpose using the values corresponding to nodular cast iron, ie, $\Delta K_{th\ int}$ = 4.5 MPa.m½ and K^{∞}_{op} = 4.10 MPa.m½. Fig. 12a gives the variations of the threshold as a function of the R ratio and the crack length. At a given R ratio, $\Delta K_{th} = \Delta K_{th\ int}$ when a is lower than a transition value a_t below which then is no crack closure effect. The transition length a_t can be calculated from the implicit expression between ΔK_o, R and $K_{op}(a)$:

$$K_{op}(a) = \frac{R}{1-R}\,\Delta K_o \qquad (3)$$

Fig. 12b is another representation of the same relationship where the variations of the threshold at various crack lengths is plotted as a function of the R ratio. This figure illustrates clearly that the short crack effects extend over physically important crack length ranges only at low R ratios in materials similar to nodular cast iron.

METALLURGICAL FACTORS

In the above discussion, it was assumed that LEFM concepts can be applied even for very small cracks, which is not necessarily true. In particular, the analysis in terms of ΔK should be limited to stage II crack growth with a stable crack front shape. For crack initiation and early stage I propagation LEFM is unlikely to be capable of characterizing crack growth in many situations. An obvious factor contributing to short crack behaviour is the grain size. Other factors as indicated by Schijve |8|

could also intervene :

(i) The front of a microcrack is more regular than the front to a macro crack.
(ii) A single slip system is required for propagating a small crack, whereas several systems are usually necessary for macrocracks.
(iii) Anisotropy effects and grain boundary structure may influence small crack behaviour.
(iv) The reversed crack tip plastic zone may be different and may induce crack closure effects function of the crack length.
(v) The roughness of the fracture surfaces may play a critical role for crack closure phenomenon.

It is expected that the importance of factors (i), (ii) and (iii) is predominant for stage I microcracks, especially in large grained materials such as several Ti alloys or cast Ni base and Fe base materials. In fine grained ferritic materials such as nodular cast iron or quenched and tempered steels, stage I extends over very small crack length ranges ($\simeq$ 10 µm). In these materials, the intrinsic threshold does not therefore reflect stage I growth only.

An attempt has been made to relate the distance l_1 (see Fig. 2) over which the short crack problem intervenes to a microstructural length (d) such as the grain size for mild steel and Al bronze, or the spacing of martensitic laths in quenched and tempered steels |11,12,20|. An empirical relationship in which $l_1 \simeq 10$ d was found. It is clear that this is an area requiring further experimental work. In particular, detailed observations of the interactions between a growing crack and grain boundaries would be useful to interpret both the intrinsic threshold and the roughness induced crack closure phenomenon.

The applicability of the simple extrapolation of stage B of the Paris law must be cautiously examined when changes in the rupture micromechanisms directly related to crack propagation occur. This is the situation which can be encountered in the presence of an environmental effect, as clearly shown by Gangloff |29,30|. This author investigated long cracks (a $\simeq$ 50 mm) and short cracks (0.1 - 0.8 mm) in high strength AISI 4340 steel tested either in moist air or in an aqueous 3% Na Cl solution. His results, given in Fig. 13, show a dramatic effect of an agressive environment on short crack F.C.G.R., even at high growth rates corresponding to stage B of the Paris law. It is unlikely that tests carried out at high R ratios on long cracks would be sufficient to evaluate the intrinsic threshold, if it exists, because of the influence of K_{Max} on crack propagation rate under such conditions.

CONCLUSIONS

1. The crack growth behaviour of short fatigue cracks is better analyzed on two-dimensional artificial short cracks than on natural short cracks, which are intrinsically three-dimensional.

2. In fine grained materials, as in ferritic steels, the short crack specificity is essentially related to crack closure effects.

3. The resistance to short crack propagation can be estimated from long crack data at high R ratios assuming that crack closure alone is responsible for the specificity of short cracks.

4. Both metallurgical and environmental effects can cause additional difficulties in predicting the short crack propagation rate.

ACKNOWLEDGMENTS

The author would like to acknowledge many fruitful discussions with the members of his research group, in particular F. MUDRY, J.L. BREAT and P. CLEMENT.

REFERENCES

1. Pearson, S., Eng. Fract. Mechanics, 7, (1975), 235.
2. El Haddad, M.H., Topper, T.H., and Smith., Eng. Fract. Mechanics, 11, (1979), 573.
3. Kitagawa, H., Takahashi, S., Suh, C.M., and Miya Shita, S., Fatigue Mechanisms, ASTM STP 675, (1979), 420.
4. Usami, S., and Shida, S., Fatigue of Eng. Materials and Structures, 1, (1979), 471.
5. Lankford, J., Fatigue of Eng. Materials and Structures, 5, (1982), 223.
6. Tanaka, K., Nakai, Y., and Yamashita, M., International Journal of Fracture, 17, (1981), 519.
7. Schijve, J., Fatigue of Eng. Materials and Structures, 5, (1982), 77.
8. Schijve, J., Fatigue Threshold, EMAS Publ., (1982), 881.
9. Bréat, J.L., Mudry, F., and Pineau, A., Fatigue of Eng. Materials and Structures, 6, (1983), 349.
10. Brown, C.W., and Hicks, M.A., Fatigue of Eng. Materials and Structures, 6, (1983), 67.
11. Taylor, D., and Knott, J.F., Metals Technology, 9, (1982), 221.
12. Taylor, D., and Knott, J.F., Fatigue of Eng. Materials and Technology, 4, (1981), 147.
13. James, M.R., and Morris, W.L., Metall. Trans., 14A, (1983), 153.
14. James, M.N., and Smith, G.C., International Journal of Fatigue, 5, (1983) 75.
15. Clément, P., and Angéli, J.P., and Pineau, A., Short crack behaviour in nodular cast iron, to appear in Fatigue of Eng. Materials and Structures (1984).
16. Miller, K.J., Fatigue of Eng. Materials and Structures, 5, (1982), 223.

17. Suresh, S. and Ritchie, R.O. The propagation of short fatigue cracks. Department of Materials Science and Mineral Engineering. University of California, Berkeley (U.S.A.), Report n°-UCB/RP/83/1014, (1983).

18. Rooke, D.P., and Cartwright, D.J., Compendum of stress intensity factors, (1974).

19. Scott, P.M., and Thorpe, T.W., Fatigue of Eng. Materials and Structures, 4, (1981), 291.

20. Taylor, D., Fatigue of Eng. Materials and Structures, 5, (1982), 305.

21. Romaniv, O.N., Siminkovitch, A.N., and Tkacha, N. Fatigue Threshold, EMAS Publ., (1982), 799.

22. Elber, W., Eng. Fracture Mechanics, 2, (1970), 37.

23. Ritchie, R.O., and Suresh, S., Metall. Trans., 13A, (1982), 937.

24. Minakawa, K., Newman, J.C., and McEvily, A.J., Fatigue of Eng. Materials and Structures, 6, (1983), 359.

25. Bignonet, A., Dias, A., and Lieurade, H.P., Mém. Scient. Revue Métallurgie, n°9, (1982), 510.

26. Morris, W.L., Metall. Trans., 8A, (1977), 589.

27. James, M.N., and Smith, G.C., Short crack behaviour in A533B and En8 steel, to appear in the Proceedings of ICF6, Conference New-Dehli, (1984).

28. Cooke, R.J., and Beevers, C.J., Materials Science and Engineering, 13, (1974), 201.

29. Gangloff, R.P., Fatigue of Eng. Materials and Structures, 4, (1981), 15.

30. Gangloff, R.P., Res Mechanica Letters, (1981), 299.

31. Usami, S., Fatigue Threshold, EMAS Publ., (1982), 205.

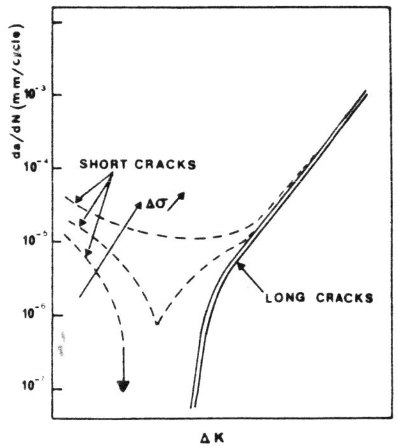

Fig. 1 - Schematic curves summarizing short fatigue cracks data. Comparison with as the results obtained on conventional long cracks specimens.

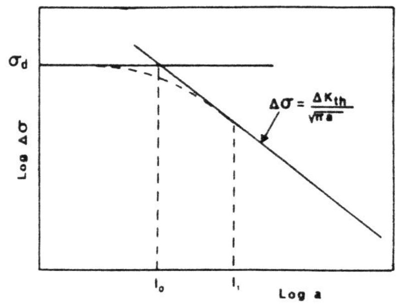

Fig. 2 - Variations of the stress amplitude to cause fatigue failure as a function of crack length. The minimum stress is assumed to be equal to zero.

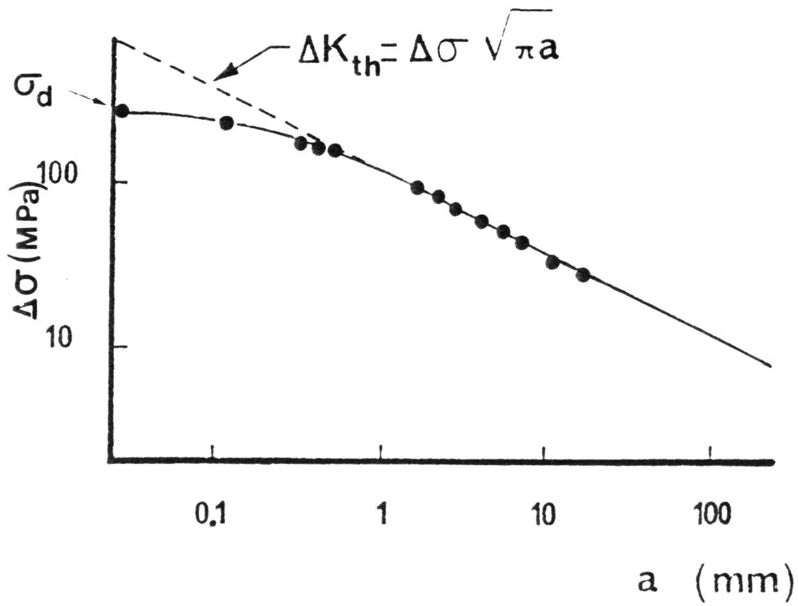

Fig. 3a - Low alloy steel tested at R = -1. Effect of crack length on stress range to cause fatigue failure (Ref. |2|).

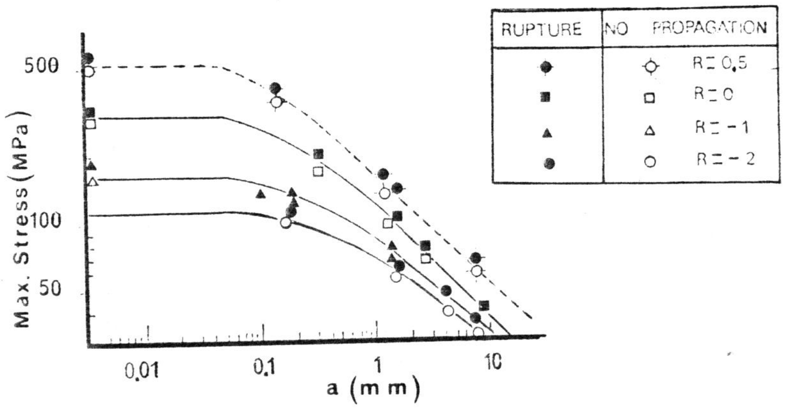

Fig. 3b - Mild steel. Variation of the maximum stress as function of effective crack length (Ref. |4|).

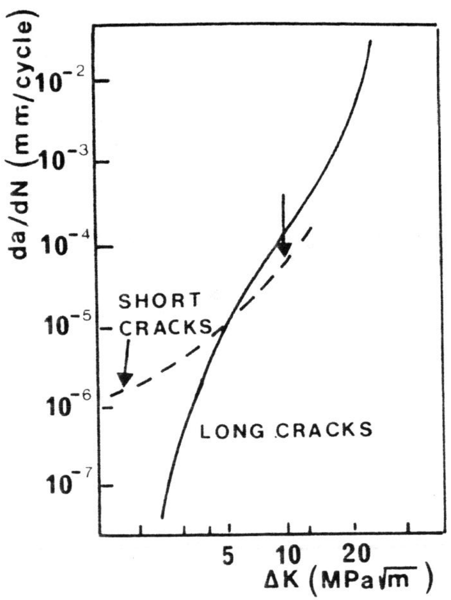

Fig. 4 - Comparison between long and short cracks data in an Al alloy (Ref. |1|). The vertical arrow indicates approximately the value of ΔK correspon-ding to a semi-circular crack such as a = c ≈ 0.25 mm.

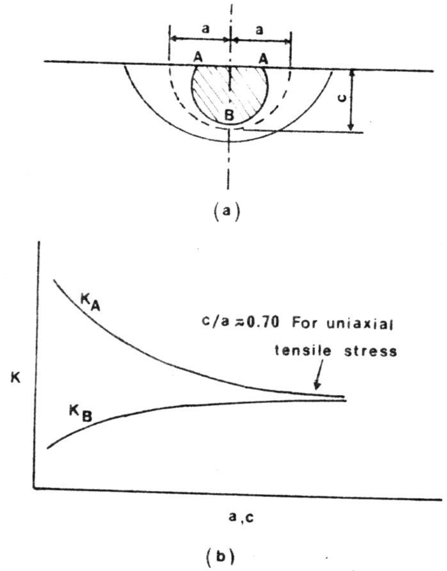

Fig. 5 - a) Section of an inclusion and successive positions of the crack front. b) Schematic variations of the stress intensity factor calculated at A and B as a function of crack dimensions.

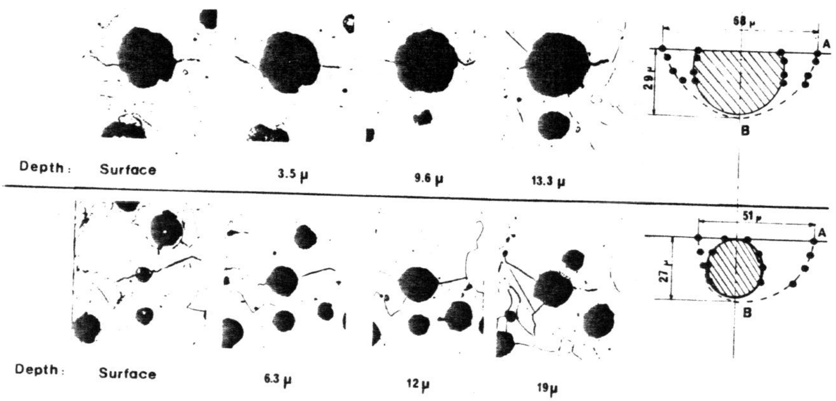

Fig. 6 - Optical micrographs prepared from successsive sections and showing the three dimensional aspects of tiny cracks initiated from graphite nodules in nodular cast iron.

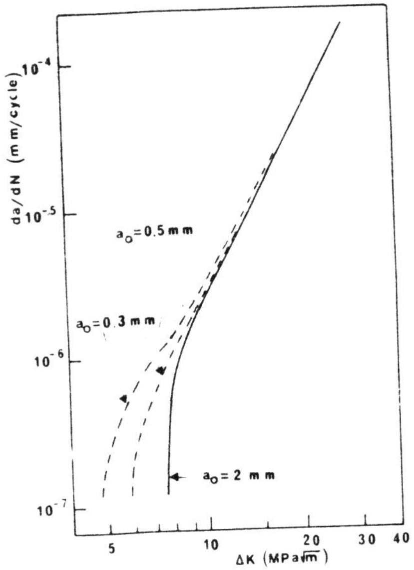

Fig. 7 - Fatigue crack propagation curves for long and short two-dimensional cracks in a mild steel. The initial dimensions of the cracks are given (Ref. |21|).

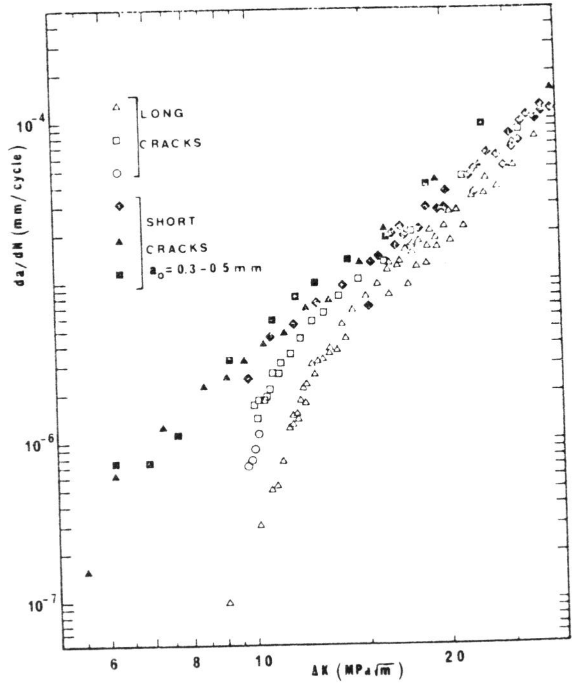

Fig. 8 - A508 steel. Crack propagation rates for long (≃ 10-20 mm) and small cracks (Ref. |9|).

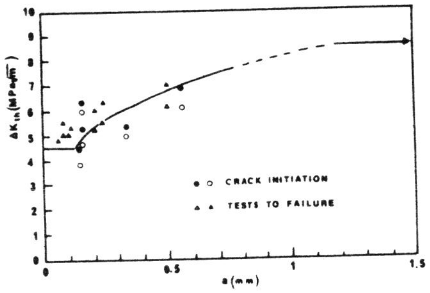

Fig. 9 - Nodular cast iron. Variation of the threshold stress intensity factor range as a function of initial crack length. The horizontal arrow corresponds to long cracks. The circles correspond to specimens instrumented for monitoring crack initiation. Tests conducted at R = 0.10.

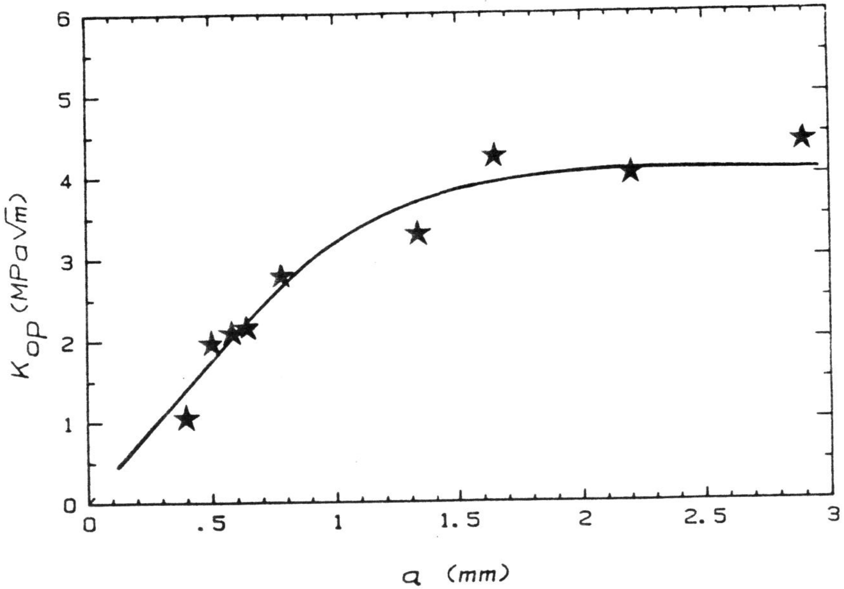

Fig. 10 - Nodular cast iron. Measurement of the opening stress intensity factor, K_{op} as a function of crack length in a specimen which contained an initial small crack of 0.4 mm.

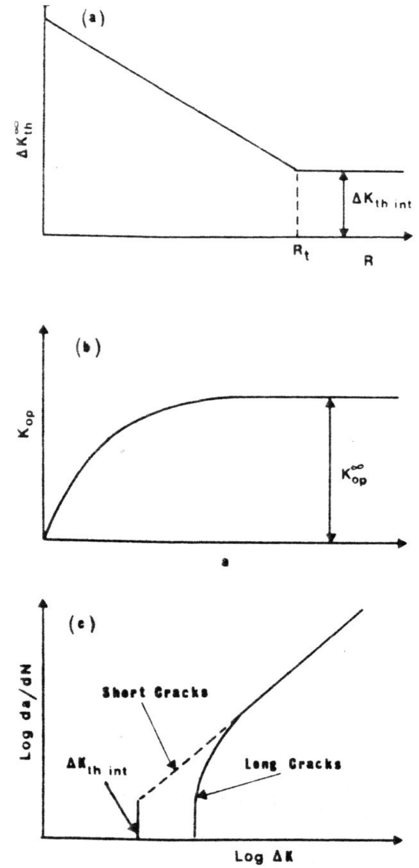

Fig. 11 - Schematic variations of a) Fatigue threshold as a function of R ratio in long crack specimens. b) K_{op} versus crack length; c) crack growth rate as a function of ΔK and initial crack length.

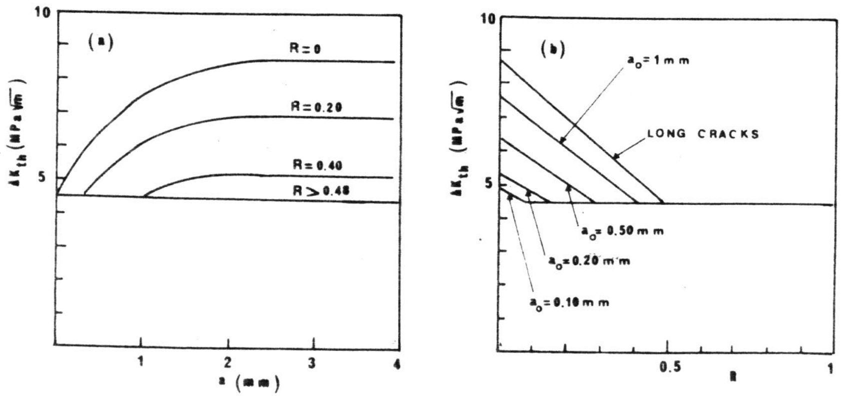

Fig. 12 - Application of crack closure effect to nodular cast iron. Variations of threshold with a) initial crack length and with b) R ratio.

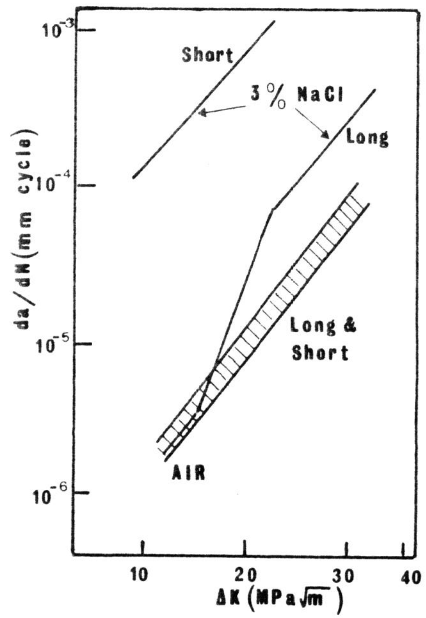

Fig. 13 - AISI 4340 Steel. Effect of environment and crack length on crack propagation rate (Ref. |29,30|.